CFD simulations and experiments for fire smoke and ventilative cooling performance in a high-rise atrium

Haohan Sha[1,2], Xin Zhang[2], Dahai Qi[2]
[1]Qingdao University of Technology, Qingdao, China
[2]University of Sherbrooke, Sherbrooke, Canada

Abstract

Atriums are popular in high-rise buildings due to their architectural features, e.g., providing sunlight. For high-rise atriums, natural ventilation (NV) is a promising technique to reduce the ventilation and cooling energy consumption. However, the fire safety issue on the NV application in atriums is a challenge. When fire occurs, the smoke can spread far away from the source in the large vertical space of atriums and threaten the occupants. To improve fire safety and promote the NV application in atriums, a novel design based on a ventilation shaft and segmentation is proposed for high-rise atriums in this study. Numerical simulations and experiments on a 1:20 small-scale model were conducted to evaluate the performance of this novel design on smoke control and NV respectively. The numerical results show that the novel design can improve the smoke control performance, which reduces the smoke layer depth. The experimental results show that the novel design can achieve better performance on ventilative cooling than the traditional design (e.g., similar or more heat removed by ventilation). This study can improve fire safety and promote the NV application in the high-rise atrium.

Introduction

High-rise buildings usually have a higher energy consumption than low/medium-rise buildings due to their high internal heat gain and the use of glazing facades (Sha, Moujahed, & Qi, 2021). It was reported that the electricity use of high-rise buildings can increase by 137% compared with the low-rise buildings (Godoy-Shimizu et al., 2018). Therefore, how to reduce cooling energy consumption in high-rise buildings has become a popular topic.

Due to the high-open space and special aesthetic environment, atriums have been a popular architectural component in high-rise buildings (Sha & Qi, 2020). Furthermore, high-rise atriums can employ natural ventilation (NV) technology to reduce the cooling energy consumption, i.e., ventilative cooling (Moosavi, Mahyuddin, Ab Ghafar, & Azzam Ismail, 2014). Previous studies showed that NV can reduce up to 86% cooling energy consumption in a high-rise atrium (Hu & Karava, 2014). NV system is effective in high-rise atriums due to buoyancy. The buoyancy force is based on the pressure difference when the indoor temperature is greater than the outdoor temperature. A larger height difference between the lower inlet opening and higher outlet opening can generate a stronger buoyancy force.

However, when a fire occurs, high-rise atriums is difficult to manage the smoke movement due to their large vertical space (Qi, Wang, & Zmeureanu, 2014). Toxic smoke will spread far away from the fire source, causing a huge number of losses, e.g., threatening occupants and damaging properties (Qi, Wang, & Zhao, 2017). To mitigate the fire safety concerns, the atrium height usually is limited and reduces the potential of NV in turn. For example, Concordia engineering and visual arts building has a high-rise atrium that is divided into five segments (Yuan, Vallianos, Athienitis, & Rao, 2018). Each segment is three floors high and is connected to other segments through the motorized openings.

Based on the fire safety concern and natural ventilation potential in the atrium, a novel design is proposed. This new NV system includes two components: a segmentation slab and a ventilation shaft, which is shown in Figure 1. The segmentation slab can divide the atrium into different segments and reduce the height of the atrium. The ventilation shaft is to maintain the NV rate of the lower segments for daily use and extract smoke during a fire. It should be noted that this study only investigated the ventilation performance in the lower segment. It assumes that the upper part will not be occupied.

A 1:20 small-scale CFD simulation and experimental model (1.5 m (L) * 0.6 m (W) *1.5 m (H)) were developed to evaluate the smoke control and ventilation performance of the novel system in this study, respectively. The experimental model is used to evaluate the ventilation performance and investigate the influence of inlet/outlet openings, which demonstrates the temperature distribution in the atrium, ventilation rate, and heat removed by ventilation. The CFD numerical models examine the smoke control performance, which shows the smoke layer heights.

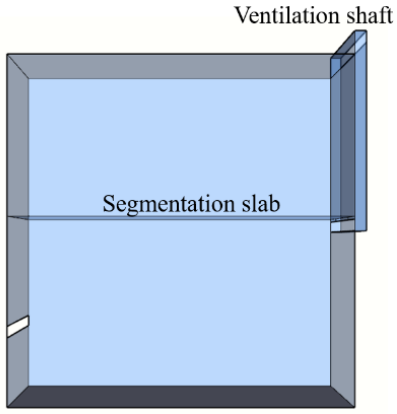

Figure 1: Perspective view of the atrium with the novel natural ventilation system.

Methodology

CFD simulation

The design of the NV system changes the atrium's structure, the mechanical exhaust systems need to be modified for the different structures. To compare the smoke control performance of the atrium with the novel NV system and traditional NV system, two corresponding mechanical exhaust systems were designed the simulated in Fire Dynamics Simulator (FDS) (K. McGrattan, Hostikka, McDermott, Floyd, & Vanella, 2019). It should be noted that these two mechanical exhaust systems are independent from the NV systems, because the NV systems are used for daily ventilation but not for smoke control.

FDS is a computational tool based on the Navier-Stokes equations. In FDS, Turbulence is modelled using Large Eddy Simulation (LES) (K. B. McGrattan, McDermott, Vanella, Hostikka, & Floyd, 2020). The fundamental governing equations in the simulations are shown as below (Sun et al., 2009), which include the continuity equation, momentum equation, energy equation, and species equation.

$$\frac{\partial \rho}{\partial t} + u \cdot \nabla \rho = -\rho \cdot \nabla u \quad (1)$$

$$\rho \left[\frac{\partial u}{\partial t} + u \cdot \nabla u \right] + \nabla \mathrm{p} = \rho g + f + \nabla \cdot \tau_{ij} \quad (2)$$

$$\frac{\partial \rho h}{\partial t} + \nabla \rho h u = \frac{D \mathrm{p}}{D t} + \dot{q'} - \nabla \cdot \mathrm{q} + \Phi \quad (3)$$

$$\frac{\partial \rho Y_l}{\partial t} + \nabla \cdot \rho Y_l u = \nabla \cdot \rho D_l \nabla Y_l + \dot{m}_l' \quad (4)$$

Where ρ is density, t is time, u is velocity vector, p is the pressure (assuming equal to the background pressure p_0), g is the acceleration of gravity f is the external force vector (excluding gravity), τ_{ij} is viscous stress tensor, h is the mass-weighted average enthalpy of the lumped species, $\dot{q'}$ is the heat release rate per unit volume, q is the heat flux vector, Φ is the dissipation function, Y_l is the mass fraction of the l th species, D_l is diffusion coefficient of l th species, $\dot{m}_l'$ is the mass-production rate per unit volume of l th species due to chemical reaction. The background pressure can be approximated with a time-dependent background pressure, which is restricted to flows with low Mach number. This means that only the density can have a large variation, but pressure cannot in the formulations. The pressure term appears to:

$$p_0(\mathrm{t}) = \rho T R \sum_l Y_l M_l = \frac{\rho T R}{M} \quad (5)$$

Where R is the universal gas constant, M is the molecular weight, T is temperature.

The two mechanical exhaust systems are based on the design fire scenario. For the fire scenario, the heat release rate (HRR) can be assumed as 2 MW (Ding, Minegishi, Hasemi, & Yamada, 2004). Since this is a 1:20 small-scale simulation, a 0.1 m (L) * 0.1 m (W) fire source with a 1.1 kW fire was simulated at the centre of the atrium bottom, which is scaled by Froude modelling (Ding et al., 2004). Furthermore, based on the HRR, the reasonable grid size can be determined by the characteristic diameter (Ji, Han, Fan, Gao, & Sun, 2013). In this study, the 0.013 m grid size was used.

For the atrium with the traditional NV system, the mechanical exhaust system was designed based on ASHRAE handbook (Klote, Milke, Turnbull, Kashef, & Ferreira, 2012). With a total volumetric flow rate of 81 L/s, this system includes six exhaust inlets which are shown in Figure 2 (a). For the atrium with the novel NV system, the new mechanical exhaust system has a total volumetric flow rate of 32 L/s, but smoke is only discharged through the ventilation shaft. Figure 2 (b) presents the new mechanical exhaust system. The different flow rates for the traditional NV system and novel NV system are caused by the different heights. According to the ASHRAE handbook (Klote et al., 2012), the design volumetric flow rate is related to the heights of the atrium. Since the novel NV system adds a segmentation slan, its required volumetric flow rate is lower than the traditional NV system. These two exhaust volumetric flow rates (81 L/s and 32 L/s) have been scaled down based on the Froude modelling due to 1:20 scaling (Klote et al., 2012).

Both of these two exhaust systems aim to maintain a 20% smoke layer depth. Considering the limitation of the makeup air velocity (1.02 m/s), the makeup air openings on the two sides of the atrium were added (0.17 m^2). For these two cases, the smoke layer heights were measured at A and B positions (see Figure 2 (a) and (b)).

The whole model was simulated in a 1.7 m (L)*0.8 m (W) * 2.2 m (H) domain with "OPEN" boundary. The "OPEN" boundary in FDS is where the fluid is allowed to enter ort exist the computational domain based on local pressure gradients. The suitable grid size of the meshes should be based on the characteristic diameter of the fire source. The

ratio of the characteristic diameter to the grid size should be within 4~16 (Liu, Liu, Xiong, Weng, & Wang, 2020). In this study, the grid size should be within 0.004 m ~0.015 m. Therefore, for balancing the simulation time and results accuracy, the 0.013 grid size was selected, and the number of meshes is 1229312. In the simulation, the smoke layer height of A and B positions are measured for making a comparison.

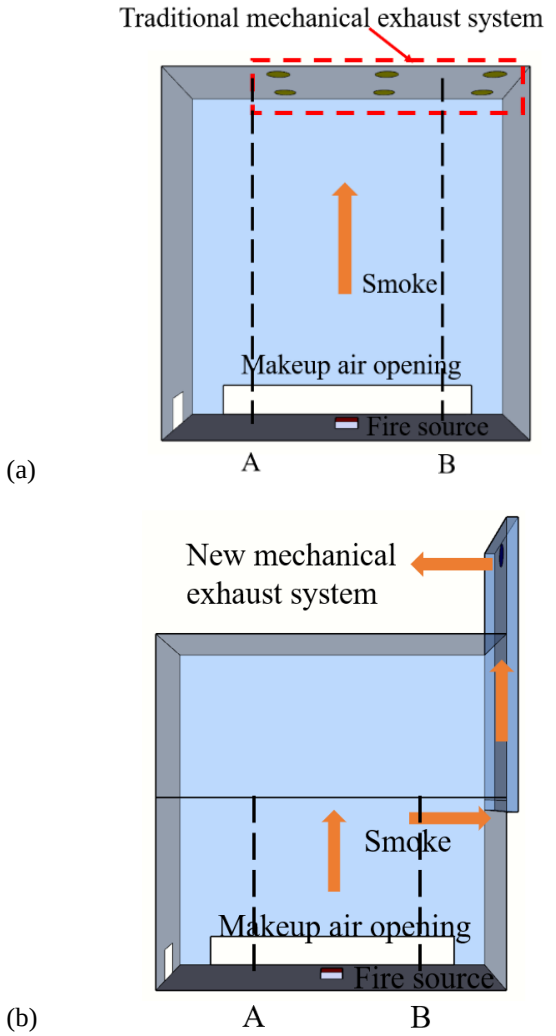

Figure 2: Perspective view of two mechanical exhaust systems (a) atrium with the traditional NV system and (b) atrium with the novel NV system.

Small-scale experiment

To compare the ventilation performance of the novel NV and the traditional NV systems, a 1:20 reduced-scale atrium model was developed by using the acrylic board, see Figure 3 (a) and (b), which has the perspective view of the models. The traditional NV system only utilizes the inlet and top outlet openings (see Figure 3(a)). The novel NV system has the segmentation and ventilation shaft (see Figure 3 (b)), which utilizes the inlet and shaft outlet openings.

The dimensions of this model are 1.5 m (L) * 0.6 m (W) *1.5 m (H). A 0.05m-Width shaft is designed at the side of the model. At 0.8 m height, a removable segmentation slab is installed, which can divide the atrium into upper and lower parts (see Figure 3 (b)). A ventilation shaft is installed at the side of the model. On the ventilation shaft, there are two openings with an area of 0.03 m^2: upper opening (0.8 m) and lower opening (1.6 m), which are used to switch the type of NV systems. Also, there are inlet (0.3 m) and outlet openings (1.6 m) on the model.

A 0.6 m (L) * 0.2 m (W) heater is placed at the centre of the model to simulate the cooling load. For the traditional NV system, the outside air flows into the atrium from the inlet opening, passes through the shaft upper opening, and finally is discharged from the outlet opening (see Figure 3 (a)). In the novel NV system, the air flows into the model from the inlet opening, passes through the shaft lower opening, and finally is discharged from the outlet (See Figure 3 (b)).

Based on the two NV systems, four cases were evaluated in this paper, which is shown as Table 1. Two different inlet/outlet opening sizes were evaluated.

Two T-type thermocouples trees were installed at A and B positions (see Figure 3 (a)). Temperature data were collected by DAQ6510 (Tektronix, 2021). The thermocouple error is 0.2 ℃ at the temperature range 18-28℃ but has an additional error of 0.03 ℃ for each ℃ outside 18-28℃, which is around 0.3 ℃ in this study. In the model with the novel NV system, two thermocouple trees are employed at the A and B positions in the lower part of the atrium. Furthermore, other two thermocouple trees were installed in the shaft (see Figure 3 (b)). Two anemometers were used to measure the air velocity at the inlet/outlet openings. The hot wire anemometer (from OMEGA HHF-SD1) with the read accuracy at around 0.1 m/s (OMEGA, 2021) was used.

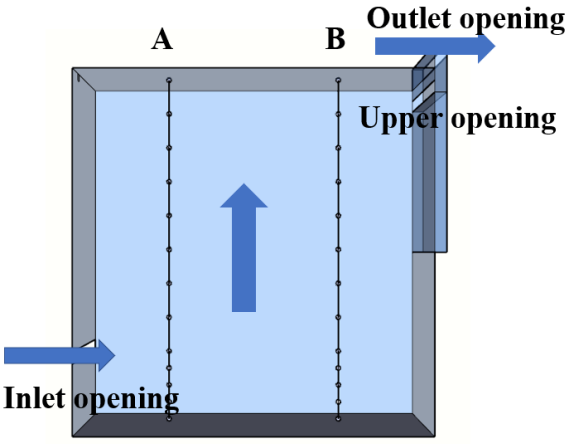

(a)

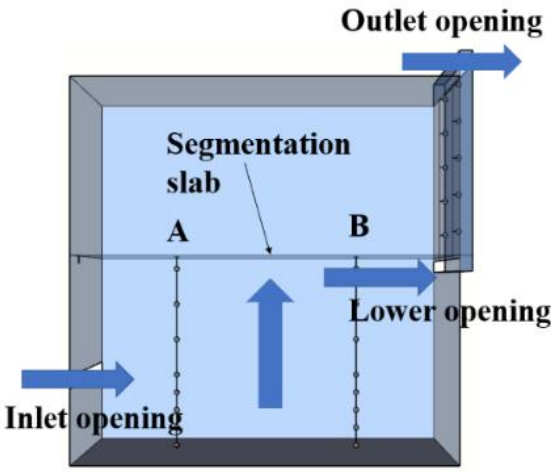

(b)

(c)

Figure 3: Arrangement of measured points in (a) traditional natural ventilation system, (b) novel natural ventilation system, and (c) experimental set-up.

Table 1. Experimental conditions for natural ventilation.

Cases	Natural ventilation system	Opening sizes (m^2)
NV1	Traditional design	0.03
NV2	Traditional design	0.015
NV3	Novel design	0.03
NV4	Novel design	0.015

Results and Discussion

Smoke control simulation

Figure 4 presents the relative smoke layer heights at A and B positions in the atrium with the traditional and novel NV system. It can be found that the results are stable within 500s, which means the smoke layer height will not reduce further. The atrium with the novel NV system has a better smoke control performance than the atrium with the traditional NV system. On the one hand, Figure 4 shows the atrium with the new NV system has a thinner smoke layer than with the traditional NV system. For example, Figure 4 (a) shows that the relative smoke layer mainly is from 0.6 to 1, i.e., the smoke layer occupies around 40% of space. However, Figure 4. (b) shows that the relative smoke layer concentrates on the heights from 0.35 to 0.55, i.e., the smoke layer occupies around 20% of the space. Furthermore, in the atrium with the novel NV system, the upper zone is totally smoke-free. On the other hand, the mechanical exhaust flow rate in the atrium with the novel NV system (81L/s) is around 2.5 times higher than in the atrium with the novel NV system (32 L/s). These results are caused by the segmentation slab. Since the atrium height reduces, less smoke is generated.

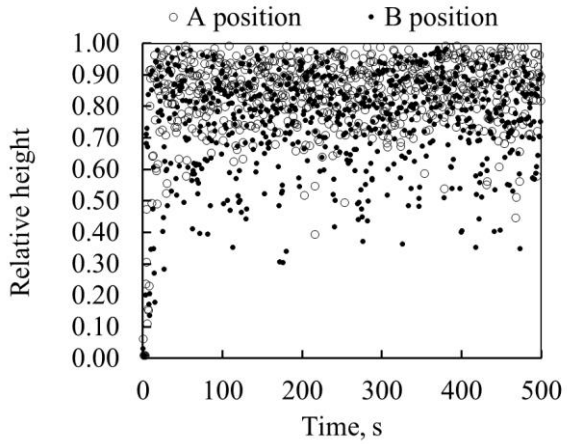

(a)

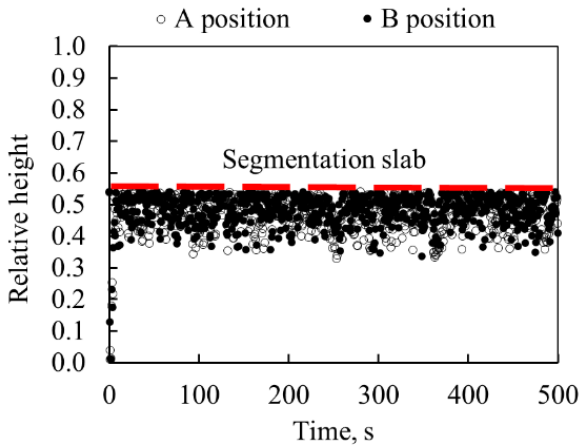

(b)

Figure 4: Relative smoke layer height at A and B positions in the atrium with (a) traditional natural ventilation system and (b) novel natural ventilation system.

Ventilative cooling experiment

Figure 5 (a) presents the measured temperature difference distribution at A, B positions and shaft for the traditional and new NV systems. In the experiment, the surrounding temperature is around 21.5 ℃. For Figure 5 (b), the temperature data over 0.8 m height in NV3 and NV4 are the temperature difference distribution in the shaft. Two points can be found in Figure 5. Firstly, when the inlet/outlet opening size is 0.03 m^2, the temperatures are very close at the bottom for the two NV systems. These results indicate the new NV system can maintain the temperature of the occupied space as low as the traditional NV system. For example, for NV1 and NV3, the temperature differences are 3℃ and 4 ℃ at the bottom (lower than 0.1 m) of A positions. The temperature differences are 4.8℃ and 5.3℃ at the bottom (lower than 0.1 m) of B positions.

Secondly, with the inlet/outlet opening size of 0.015 m^2, the temperature at B position in the novel NV system is lower than that in the traditional NV system. For example, the temperature differences are 8.7℃ and 6.3℃ at the bottom (lower than 0.1 m) of B positions for NV2 and NV 4. These results indicate that the novel NV system can have a cooler occupied space than the traditional NV system.

To further investigate the ventilation performance of two NV systems, Fig. 6 presents the measured mass flow rate and the calculated heat transfer by ventilation. It was found that compared with the traditional NV system (NV1 and NV2), the mass flow rate by ventilation in the new NV system increases 22% (NV3) and 2% (NV4) respectively. Furthermore, the heat removed by ventilation in the novel NV system is close or higher than in the traditional NV system. For example, with the 0.03 m^2 inlet/outlet opening the heat transfer by ventilative cooling in NV 3 increases by 21% compared with NV1. With the 0.015 m^2 inlet/outlet opening, the heats transferred by ventilative cooling in NV2 and NV4 are almost same.

Although a smaller opening reduces the ventilative cooling capacity, the temperature in the occupied space in the novel NV system is lower than in the traditional NV system. This difference may be caused by the heat transfer through the wall and airflow pattern. Therefore, the effects of opening size and heat transfer through the wall require further investigation in future.

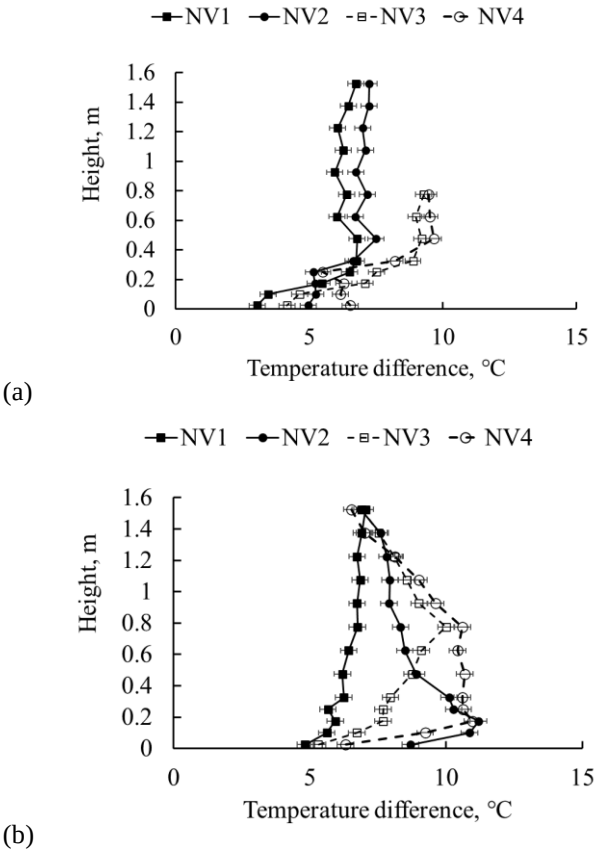

Figure 5: Temperature difference distribution in the natural ventilation experiments at (a) A position and (b) B position and shaft.

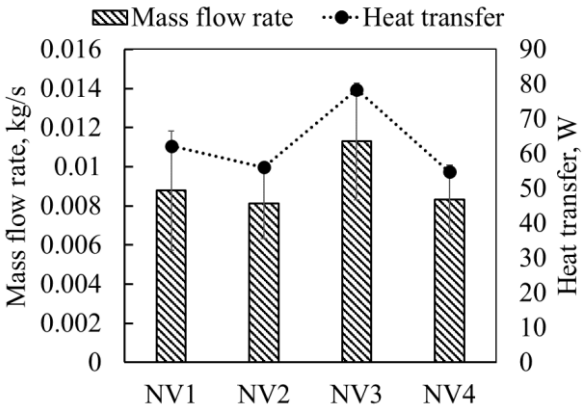

Figure 6: Measured mass flow rates and calculated heat transfer by ventilation in the experiments.

Conclusion

This study proposes a novel NV system in a high-rise atrium. Its performance on the smoke control and ventilative cooling were evaluated by the 1:20 small-scale CFD simulations and small-scale experiments. The CFD simulations show that this novel NV system can reduce the relative smoke layer depth (reduce 20%) which reduces smoke exposure to occupants and building materials. The

experiment shows that when the inlet/outlet opening sizes are 0.03 m^2, the novel NV system can remove more heat than the traditional NV system (increase by 21%), i.e., achieving better ventilative cooling performance. When the inlet/outlet opening sizes are 0.015 m^2, the novel NV system cannot remove more heat than the traditional NV system, but still maintain a low temperature at the bottom. In future, the detailed airflow pattern of this novel NV system, parametric study, and the heat transfer through the wall should be further investigated its ventilative cooling performance.

Acknowledgement

This work was supported by the Start-up Fund of the Université de Sherbrooke (UdeS) and Discovery Grants of Natural Sciences and Engineering Research Council of Canada (NSERC) (Grant number: RGPIN-2019-05824). The technical support in developing the small-scale experimental atrium model from Mr. Frédéric Turcotte (Département de génie civil et de génie du bâtiment of UdeS) is also acknowledged.

References

Ding, W., Minegishi, Y., Hasemi, Y., & Yamada, T. (2004). Smoke control based on a solar-assisted natural ventilation system. *Building and Environment*, *39*, 775–782. https://doi.org/10.1016/j.buildenv.2004.01.002

Godoy-Shimizu, D., Steadman, P., Hamilton, I., Donn, M., Evans, S., Moreno, G., & Shayesteh, H. (2018). Energy use and height in office buildings. *Building Research and Information*, *46*(8), 845–863. https://doi.org/10.1080/09613218.2018.1479927

Hu, J., & Karava, P. (2014). Model predictive control strategies for buildings with mixed-mode cooling. *Building and Environment*, *71*, 233–244. Retrieved from https://doi.org/10.1016/j.buildenv.2013.09.005

Ji, J., Han, J. Y., Fan, C. G., Gao, Z. H., & Sun, J. H. (2013). Influence of cross-sectional area and aspect ratio of shaft on natural ventilation in urban road tunnel. *International Journal of Heat and Mass Transfer*, *67*, 420–431. https://doi.org/10.1016/j.ijheatmasstransfer.2013.08.033

Klote, J. H., Milke, J. A., Turnbull, P. G., Kashef, A., & Ferreira, M. J. (2012). *Handbook of Smoke Control Engineering*. Atlanta: American Society of Heating Refrigerating and Air-Conditioning Engineers.

Liu, F., Liu, Y., Xiong, K., Weng, M., & Wang, J. (2020). Experimental and numerical study on the smoke movement and smoke control strategy in a hub station fire. *Tunnelling and Underground Space Technology*, *96*(November 2019), 103177. https://doi.org/10.1016/j.tust.2019.103177

McGrattan, K. B., McDermott, R., Vanella, M., Hostikka, S., & Floyd, J. (2020). Fire dynamics simulator Technical Reference Guide Volume 1: Mathematical Model, *1*. Retrieved from https://nvlpubs.nist.gov/nistpubs/Legacy/SP/nistspecialpublication1018.pdf

McGrattan, K., Hostikka, S., McDermott, R., Floyd, J., & Vanella, M. (2019). *FDS user guide*. *National Institute of Standards and Technology*. https://doi.org/10.6028/NIST.SP.1019

Moosavi, L., Mahyuddin, N., Ab Ghafar, N., & Azzam Ismail, M. (2014). Thermal performance of atria: An overview of natural ventilation effective designs. *Renewable and Sustainable Energy Reviews*, *34*, 654–670. Retrieved from https://doi.org/10.1016/j.rser.2014.02.035

OMEGA. (2021). *Hot wire anemometer*. https://doi.org/10.1533/9780857093868.67

Qi, D., Wang, L., & Zhao, G. (2017). Froude-Stanton modeling of heat and mass transfer in large vertical spaces of high-rise buildings. *International Journal of Heat and Mass Transfer*, *115*, 706–716. https://doi.org/10.1016/j.ijheatmasstransfer.2017.08.030

Qi, D., Wang, L., & Zmeureanu, R. (2014). An analytical model of heat and mass transfer through non-adiabatic high-rise shafts during fires. *International Journal of Heat and Mass Transfer*, *72*, 585–594.

Sha, H., Moujahed, M., & Qi, D. (2021). Machine learning-based cooling load prediction and optimal control for mechanical ventilative cooling in high-rise buildings. *Energy and Buildings*, *242*, 110980. Retrieved from https://doi.org/10.1016/j.enbuild.2021.110980

Sha, H., & Qi, D. (2020). A review of high-rise ventilation for energy efficiency and safety. *Sustainable Cities and Society*, *54*, 101971. https://doi.org/10.1016/j.scs.2019.101971

Sun, X. Q., Hu, L. H., Li, Y. Z., Huo, R., Chow, W. K., Fong, N. K., … Li, K. Y. (2009). Studies on smoke movement in stairwell induced by an adjacent compartment fire. *Applied Thermal Engineering*, *29*(13), 2757–2765. https://doi.org/10.1016/j.applthermaleng.2009.01.009

Tektronix. (2021). *DAQ6510 Data Acquisition and Logging , Multimeter System*. Retrieved from https://www.tek.com/en/products/keithley/digital-multimeter/keithley-daq6510

Yuan, S., Vallianos, C., Athienitis, A., & Rao, J. (2018). A study of hybrid ventilation in an institutional building for predictive control. *Building and Environment*, *128*, 1–11. Retrieved from https://doi.org/10.1016/j.buildenv.2017.11.008